Ferrous and ferric differentially deteriorate proliferation and differentiation of osteoblast-like UMR-106 cells

Kornkamon Lertsuwan · Ketsaraporn Nammultriputtar · Supanan Nanthawuttiphan ·
Supathra Phoaubon · Jomnarong Lertsuwan · Jirawan Thongbunchoo ·
Kannikar Wongdee · Narattaphol Charoenphandhu

Abstract The association between iron overload and osteoporosis has been found in many diseases, such as hemochromatosis, β-thalassemia and sickle cell anemia with multiple blood transfusion. One of the contributing factors is iron toxicity to osteoblasts. Some studies showed the negative effects of iron on osteoblasts; however, the effects of two biological available iron species, i.e., ferric and ferrous, on osteoblasts are elusive. Since most intracellular ionized iron is ferric, osteoblasts was hypothesized to be more responsive to ferric iron. Herein, ferric ammonium citrate (FAC) and ferrous ammonium sulfate (FAS) were used as ferric and ferrous donors. Our results showed that both iron species suppressed cell survival and proliferation. Both also induced osteoblast cell death consistent with the higher levels of cleaved caspase 3 and caspase 7 in osteoblasts, indicating that iron induced osteoblast apoptosis. Iron treatments led to the elevated intracellular iron in osteoblasts as determined by atomic absorption spectrophotometry, thereby leading to a decreased expression of genes for cellular iron import and increased expression of genes for cellular iron export. Effects of FAC and FAS on osteoblast differentiation were determined by the activity of alkaline phosphatase (ALP). The lower ALP activity from osteoblast with iron exposure was found. In addition, ferric and ferrous differentially induced osteoblastic and osteoblast-derived osteoclastogenic gene expression alterations in osteoblast. Even though both iron species had

K. Lertsuwan · S. Nanthawuttiphan · S. Phoaubon
Department of Biochemistry, Faculty of Science, Mahidol
University, Bangkok, Thailand

K. Lertsuwan · K. Nammultriputtar · J. Thongbunchoo ·
K. Wongdee · N. Charoenphandhu
Center of Calcium and Bone Research (COCAB), Faculty
of Science, Mahidol University, Bangkok, Thailand

K. Nammultriputtar · J. Thongbunchoo ·
N. Charoenphandhu (✉)
Department of Physiology, Faculty of Science, Mahidol
University, Rama VI Road, Bangkok 10400, Thailand
e-mail: naratt@narattsys.com

N. Charoenphandhu
Institute of Molecular Biosciences, Mahidol University,
Nakhon Pathom, Thailand

J. Lertsuwan
Laboratory of Chemical Carcinogenesis, Chulabhorn
Research Institute, Bangkok, Thailand

K. Wongdee
Faculty of Allied Health Sciences, Burapha University,
Chonburi, Thailand

N. Charoenphandhu
The Academy of Science, The Royal Society of Thailand,
Dusit, Bangkok 10300, Thailand

similar effects on osteoblast cell survival and differentiation, the overall effects were markedly stronger in FAC-treated groups, suggesting that osteoblasts were more sensitive to ferric than ferrous.

Introduction

Iron is one of the most essential elements found in organisms. It functions as the crucial components in many biochemical molecules, such as in iron-sulfur cluster containing proteins and in the heme group of oxygen transporting-storing proteins, hemoglobin and myoglobin. Iron enters our body in one of the two forms, i.e., ferrous (Fe^{2+}) and ferric (Fe^{3+}). In enterocytes, heme-coupled ferrous can be transported into the cell via heme carrier protein (HCP1), and the free ferrous can be transported via divalent metal transporter 1 (DMT1). In contrast to a straightforward transport mechanism for ferrous, ferric from vegetables and grains needs to be reduced by ferric reductase, duodenal cytochrome b (Dcytb), to ferrous before being imported to the cell via DMT1. Ferrous can be exported out of enterocyte via ferroportin (Fpn), and is later oxidized back to ferric by the activity of oxidase enzyme, ceruloplasmin (Cp), and transported in circulation with transferrin. When transferrin-coupled iron reaches the target cells, it can be taken up by the cells via transferrin receptor-mediated endocytosis. Ferric will be released, reduced back to ferrous by ferric reductase Steap3 and exported out of the endocytic vesicle via DMT-1, respectively (MacKenzie et al. 2008; McKie et al. 2001). While the mechanism of iron uptake has been well elucidated in enterocytes and some other cell types, such as macrophages, an ability to import iron and the transport mechanism for osteoblasts are largely unknown.

Regardless to their vital roles in biological systems, excess amount of iron can become toxic to cells. For bone cells, it has been shown that iron negatively affected osteoblast survival, differentiation and mineralization, but had stimulatory effects on osteoclast development (Chen et al. 2015; Tian et al. 2016; Tsay et al. 2010; Zarjou et al. 2010; Zhao et al. 2014). Not surprisingly, osteoporosis is a common complication in several diseases with iron overload including β-thalassemia and hemochromatosis. Disease-associated osteoporosis may worsen patients' conditions, leading to immobility or even mortality from severe fracture. Therefore, knowing the potential factor governing iron-overload-induced osteoporosis would be highly beneficial for specialized drug development for this condition. Even though some investigators have reported the adverse effects of ferric on osteoblast survival and differentiation, the differential effects of ferrous and ferric on bone microenvironment have not been illustrated. High dose of ferric nitrate has been shown to suppress rat osteoblast cell (UMR-106) proliferation, protein synthesis and ALP activity (Diamond et al. 1991). Ferric in a form of ferric ammonium citrate (FAC) was also widely used to test the effects of ferric on osteoblasts. Several groups reported that FAC treatment decreased cell viability, collagen I expression and ALP activity in mouse osteoblast (MC3T3-E1) and human osteoblast (hFOB1.19) cells (He et al. 2013; Tian et al. 2016; Yamasaki and Hagiwara 2009). On the other hand, the negative effects of iron on osteoblast were also found from ferrous exposure. Another study showed that ferrous in a form of ferrous sulfate also inhibited osteoblastic gene expression and induced cell apoptosis in fetal rat-derived calvarial culture (Messer et al. 2009). In addition, another investigator showed that FAC and ferritin ferroxidase suppressed osteoblast differentiation and extracellular matrix calcium deposition in human osteosarcoma 143-B cells, suggesting the potential mechanism of iron-mediated osteoblast suppression via ferritin ferroxidase activity (Zarjou et al. 2010). Interestingly, the comparative studies of the two iron species on osteoblast have not been elucidated.

Since there are two major iron species in biological system, i.e., ferrous and ferric, our comparative study is crucial for specialized therapy targeting the iron specie that causes more detrimental effects on iron overload-induced osteoporosis. Accordingly, this study is the very first study to compare the effects of ferric and ferrous on osteoblast cell proliferation and differentiation. Specifically, the effects of the two iron forms on osteoblast survival, proliferation, function as well as the expression of osteoblastic genes,

osteoclastogenic genes and genes for iron transporters upon ferric and ferrous exposure were investigated.

Materials and methods

Cell culture and reagents

UMR-106 cells (American Type Culture Collection, ATCC, no. CRL-1661) were purchased from ATCC, and were maintained in Dulbecco's modified Eagle's medium (DMEM) (Sigma, MO, USA) supplemented with 10% fetal bovine serum (FBS) (PAA Laboratories, Pasching, Austria), and 100 U/ml penicillin–streptomycin (Gibco, NY, USA). They were grown at 37 °C with 5% CO_2 and subcultured according to ATCC's protocol. Ferric ammonium citrate (FAC) (Sigma) was used as ferric treatment, and ferrous ammonium sulfate (FAS) (Sigma) was used as ferrous treatment. Unless otherwise specified, the treatments were refreshed everyday by half changing the treatment containing media.

Cell viability assay

Osteoblastic UMR-106 cells were plated at 2500 cells/well in 96-well tissue culture plate (Corning, NY, USA). Twenty-four hours after plating, the cells were treated with escalating concentration of FAC or FAS ranging from 0 to 800 μM for 24, 48 or 72 h. After the treatment period, cell viability was measured by using MTT (3-(4,5-dimethylthiazol-2-yl)-2,5-diphenyltetrazolium bromide) assay. In short, MTT (Sigma Aldrich, MO, USA) was added to each well to achieve a final concentration of 1 mg/ml. The cells were then incubated at 37 °C for 3 h. After that, formazan dissolving solution containing 10% SDS (Sigma Aldrich, MO, USA) in 50% N,N-dimethyl-formamide (DaeJung, Gyeonggi-do, South Korea) to dissolve MTT product, formazan. The absorbance of each well representing cell viability was determined at 590 nm by a microplate reader (Model 1420; Wallac, MA, USA).

BrdU assay

Cell proliferation was determined by BrdU Cell Proliferation Assay Kit (Cell signaling technology, Inc., MA, USA). UMR-106 cells were plated in 96-well plate (Corning, NY, USA) by seeding density 2500 cells/well. After plating for 24 h, cells were treated with 5-bromo-2′-deoxyuridine (BrdU) in culture media containing iron treatment (FAC or FAS) at concentrations of 0, 1, 3, 10, 30, 100, 300 and 1000 μM for 24 h. During cell proliferation, BrdU acts as pyrimidine analog incorporated into the newly synthesized DNA of proliferating cells by replacing thymidine. After being treated, cells were fixed with fixing solution and followed by adding BrdU mouse antibody and anti-mouse IgG HRP-linked antibody to detect the incorporated BrdU. Then, the HRP-substrate, TMB (3,3′,5,5′-tetramethylbenzidine) was added to develop color, the intensity of which was quantified at 450 nm to determine the proportional BrdU incorporation that could directly indicate cell proliferation.

Live/dead cell viability assay

UMR-106 cells were plated at 1×10^5 cells/well in 6-well tissue culture plate (Corning, NY, USA). After plating for 24 h, cells were treated with 0, 100, 200 or 300 μM of FAC or FAS for 72 h. After that, the cells were simultaneously labeled with calcein AM and ethidium homodimer using Live/dead viability/cytotoxicity kit for mammalian cells (Invitrogen, CA, USA) to stain live and dead cells, respectively. The labeled cells were incubated at 37 °C for 30 min. After 30 min incubation, the pictures from seven different fields in each treatment were visualized and captured under fluorescent microscope (model BX53; Olympus Corporation, Tokyo, Japan). The quantification was done by using cellSens software (Olympus Corporation, Tokyo, Japan) to measure pixel coverage and fluorescent intensity for green (living cells) and red (dead cells) to obtain average dead/live ratio in each treatment.

Western blot analysis

Cells were plated at 4.2×10^5 cells/well in 6-well tissue culture plate (Greiner, Kremsmünster, Austria). Cells were treated with 0, 100, 200 or 300 μM of FAC and FAS for 72 h before collecting cell pellets by scraping. Cell pellets were lysed for 45 min in modified radioimmunoassay precipitation (RIPA) buffer containing 50 mM Tris–HCl (DaeJung, Gyeonggi-do, South Korea) pH 7.4, 1% Triton

X-100, 0.25% deoxycholate, 150 mM NaCl (DaeJung, Gyeonggi-do, South Korea) supplemented with Roche complete Minitabs (Roche, IN, USA) at supplier's recommended concentration. Protein concentration of the samples was measured by using BCA protein assay kit (Thermo scientific, MA, USA). Twenty-five micrograms of proteins were subjected to SDS-PAGE using 4–20% Bis–Tris polyacrylamide gels. The proteins were transferred to nitrocellulose membrane (GE, Little Chalfont, United Kingdom). Membranes were blocked for 1.5 h at room temperature in blocking buffer containing 4% w/v bovine serum albumin (BSA) in 0.1% v/v Tween 20 in Tris buffer saline (TBST). All blots were incubated in primary antibody and secondary antibody diluted in blocking buffer at 4 °C overnight and at room temperature for 75 min, respectively. Primary antibodies used in this experiment included rabbit anti-cleaved caspase-3 (Asp175) monoclonal antibody (9964, Cell Signaling Technology, MA, USA), rabbit anti-cleaved caspase-7 (Asp198) monoclonal antibody (8438, Cell Signaling Technology, MA, USA), rabbit anti-actin monoclonal antibody (A2066, Sigma Aldrich, MO, USA). Secondary antibody was goat anti-rabbit IgG conjugated with horseradish peroxidase (7074, Cell Signaling Technology, MA, USA). Proteins were visualized by enhanced chemiluminescence (ECL) (Millipore, MA, USA) and exposed to Hyperfilm (GE Healthcare, Boston, MA, USA).

Intracellular iron concentration measurement

Measurement intracellular iron concentration was done by flame atomic absorption spectroscopy (FAAS). UMR-106 cells were plated in 12-well plate (Corning, NY, USA) by seeding density 210,000 cells/well; 24 h after plating, cells were treated FAC or FAS at the concentration of 0, 100, 200 and 300 μM for 24 h. The cells were collected by washing twice in $1\times$ phosphate buffer saline (PBS) before gently scraped with cell scraper (Corning, NY, USA) in PBS. After centrifugation at 7000 rpm for 15 min, the pellet was resuspended in 500 μL of ultrapure water for a brief sonication (Li et al. 2016). Then the samples were digested with 65% nitric acid (HNO_3) and hydrogen peroxide (H_2O_2) by Ethos UP MAXI-44 microwave digester (Milestone, CT, USA). After digestion, iron concentration was measured by FAAS (PinAAcle 900T Atomic Absorption Spectrometer, PerkinElmer,

Waltham, MA, USA). In addition, the protein content of the samples was measured by bicinchoninic acid assay and was used to normalize intracellular iron concentration, as described by Noble and Bailey (2009) (Noble and Bailey 2009).

Quantitative reverse transcription polymerase chain reaction (qRT-PCR)

UMR-106 cells were plated at 4.2×10^5 cells/well in 6-well tissue culture plate (Greiner, Kremsmünster, Austria). Unless otherwise stated, cells were treated with either FAC or FAS at their half maximal inhibitory concentration (IC_{50}; determined by the experiments in Fig. 1) for 24 h before collecting cell pellets by scraping. Total cellular RNA from cell lysates was extracted by using TRIzol reagent (Invitrogen, CA, USA) according to manufacturer's instruction. Following extraction, RNA was treated with RNAse-free DNase I (Roche, IN, USA) according to manufacturer's protocol. RNA quality and quantity were analyzed spectrophotometrically by using Nano-Drop-2000c spectrophotometer (Thermo Scientific, MA, USA) and electrophoretically by using 0.8% v/w agarose gel in 0.5x Tris–acetate (TAE) buffer. One microgram of RNA was converted to cDNA by using iScript cDNA synthesis kit (Bio-rad, CA, USA) with the thermal cycler (model MyCycler; Bio-rad, CA, USA). qRT-PCR was operated by Bio-rad MiniOpticon using SsoFast EvaGreen Supermix (Bio-rad, CA, USA) according to manufacturer's recommendation. PCR was performed at 95 °C for 40 s (enzyme activation and DNA denaturation), annealing temperature (Table 1) for 30 s (annealing), 65 °C for 5 s and 95 °C for 30 s (melting curve construction). Relative expression levels of the genes mentioned in Table 1 were calculated from $2^{-\Delta Ct}$ values to the housekeeping gene [hypoxanthine phosphoribosyltransferase 1 (Hprt1) or β-actin], and normalized by control to obtain $2^{-\Delta\Delta Ct}$.

Alkaline phosphatase activity assay (ALP assay)

UMR-106 cells were plated in 12-well plate (Corning, NY, USA) at seeding density 210,000 cells/well. Twenty-four hours after plating, cells were treated with FAC or FAS at concentration 0, 100, 200, 300 μM for 24 h and collected by washing twice in PBS before gently scraped with cell scraper (Corning,
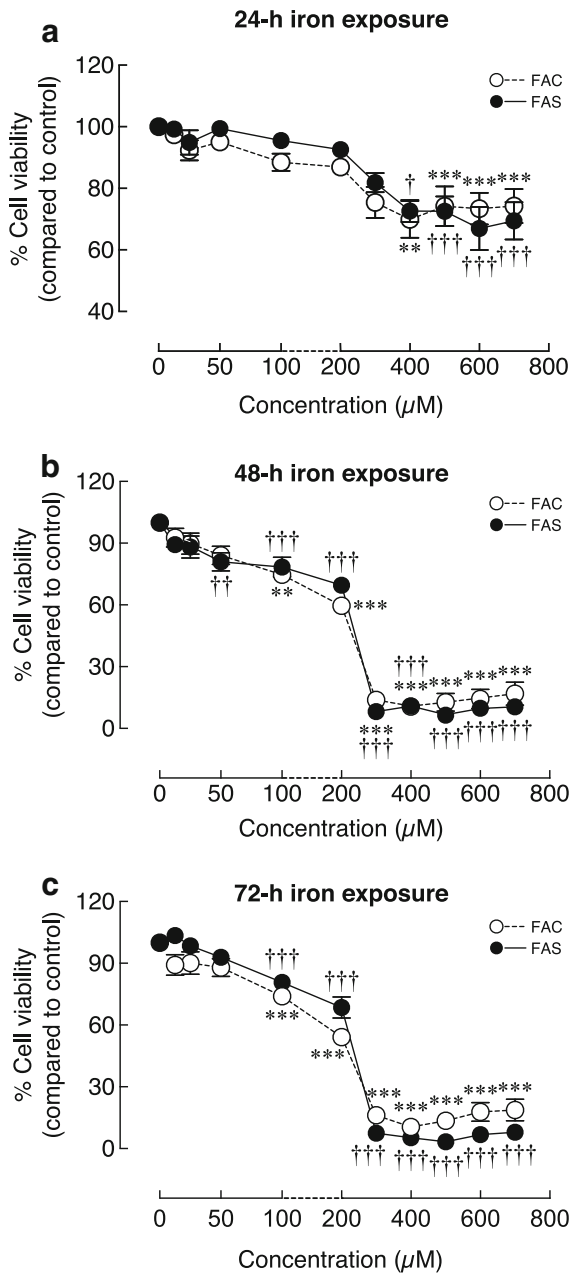
24-h iron exposure

48-h iron exposure

72-h iron exposure

Fig. 1 Effects of FAC and FAS on osteoblast cell survival after iron exposure for 24 h (**a**), 48 h (**b**) and 72 h (**c**). Both FAC and FAS treatments led to decreased osteoblast cell survival in dose dependent manner. (**P < 0.01, ***P < 0.001 as compared to control in FAC treated groups; †P < 0.05, ††P < 0.01, ††† P < 0.001, as compared to control in FAS treated group; experiments were performed in 4 biological replicates each with 3 technical repeats)

NY, USA) in PBS. After centrifugation at 7000 rpm for 15 min, the pellet was resuspended in 250 μL of lysis buffer (1% Triton X-100 in 50 mM Tris–HCl pH

7.6) for a brief sonication. In addition, the protein content of samples was measured by BCA assay (Noble and Bailey 2009) to normalize ALP activity.

To determine effects of iron on osteoblast differentiation by measurement alkaline phosphatase activity (ALP activity), 100 μL of the sample content was added into 96 well plate and incubated with 20 μL of 40 nM p-nitrophenyl phosphate (phosphatase substrate) (Sigma Aldrich, MO, USA) for 10–30 min at 37 °C. To stop reaction, 0.5 M NaOH 20 μL was added and mixed briefly before measurement the OD at 405 nm shortly after the mixing. The proportion of ALP activity was determined by the color changed from the reduction of phosphatase substrate from colorless to yellow. The quantitative of ALP activity was normalized to protein content and control.

Results

Ferrous and ferric iron differentially inhibited osteoblast cell survival

UMR-106 cells were used to determine the effects of ferric and ferrous iron on osteoblastic cell growth. The cells were treated with ferrous (FAS) or ferric (FAC) at the final concentration of iron at 0, 25, 50, 75, 100, 200, 400, 600 or 800 μM. Cells were treated with different iron species for 24, 48 or 72 h, after which the cell viability of each group was determined by MTT assay normalized to control (0 μM of treatment). Our results showed that both ferric and ferrous had a negative effect on osteoblast cell survival in a dose-dependent manner (Fig. 1). After 24-h treatment, all conditions could not suppress UMR-106 cell growth more than 50%. Even with the highest dose used in these experiments (800 μM), cell viability of UMR-106 dropped by 25.74 and 30.56% for FAC and FAS, respectively (Fig. 1a). At 48 and 72 h after treatment, UMR-106 cells responded to FAS and FAC in a similar pattern. UMR-106 cell survival reduced drastically with the treatment concentration higher than 200 μM to achieve the half maximal inhibitory concentration (IC_{50}) at 221.64 and 232.35 μM of FAC and FAS treatment after 48 h (Fig. 1b). The cells showed slightly lower IC_{50} after 72 h of iron treatments for both iron species. The IC_{50} of iron on UMR-106 cell survival at 72 h was 211.45 and 229.76 μM

Table 1 *Rattus norvegicus* primers used in the qRT-PCR experiments

Gene	Accession no.	Primer (forward/reverse)	Annealing temperature (°C)
Iron transport			
Transferrin receptor 1 (TfR1)	NM_022712	5′–ATACGTTCCCCGTTGTTGAGG–3′	52.00
		5′–GGCGGAAACTGAGTATGGTTGA–3′	
Transferrin receptor 2 (TfR2)	NM_001105916	5′–AGCTGGGACGGAGGTGACTT–3′	55.00
		5′–TCCAGGCTCACGTACACAACA–3′	
Divalent metal transporter 1 (DMT1)	NM_013173	5′–GCTGAGCGAAGATACCAGCG–3′	53.00
		5′–TGTGCAACGGCACATACTTG–3′	
Ferroportin (Fpn)	XM_017596804	5′–TTCCGCACTTTTCGAGATGG–3′	52.00
		5′–TACAGTCGAAGCCCAGGACTGT–3′	
Duodenal cytochrome B1 (DCytb1)	NM_001011954	5′–TCCTGAGAGCGATTGTGTTG–3′	50.00
		5′–TTAATGGGGCATAGCCAGAG–3′	
Ceruloplasmin (Cp)	XM_008760859	5′–TCCACTGCCATGTGACTGAC–3′	51.00
		5′–AACAACGTCATTGTGCTCGT–3′	
Hephaestin (Heph)	XM_006257049	5′–CACATTTTTCCAGCCACCTT–3′	50.00
		5′–TGACGAACTTTGCCTGTGAG–3′	
Homeostatic iron regulator (HFE)	NM_010424	5′–CAGCCTCTCACTGCCACT–3′	51.00
		5′–AGTGTGTCCCCTCCAAGT–3′	
Osteogenic differentiation factor			
Runt-related transcription factor 2 (Runx2)	NM_053470	5′–TAACGGTCTTCACAAATCCTC–3′	54.00
		5′–GGCGGTCAGAGAACAAACTA–3′	
Osteocalcin (OCN)	J04500	5′–CACAGGGAGGTGTGTGAG–3′	57.00
		5′–TGTGCCGTCCATACTTTC–3′	
Ephrin type-B receptor 4 (EphB4)	NM_010144	5′–GTGTATGCCACGATACGCTT–3′	50.85
		5′–ACTGTGTCCACCTTGATGTAGG–3′	
Ephrin B2 (Ephrin B2)	NM_001107328	5′–AACACTCTCCACAGCACACG–3′	52.30
		5′–TGGGCAGAAGACACTGTCTG–3′	
Osteoprotegerin (OPG)	NM_012870	5′–ATTGGCTGAGTGTTCTGGT–3′	50.28
		5′–CTGGTCTCTGTTTTGATGC–3′	
Cyclooxygenase2 (COX2)	NM_017232	5′–TATCAGGTCATCGGTGGAGAG–3′	53.50
		5′–CGAAGCCAGATGGTAGCATAC–3′	
Osteoclastogenic differentiation factor			
Receptor activator of nuclear factor κB ligand (RANKL)	NM_057149	5′–TCGCTCTGTTCCTGTACT–3′	47.35
		5′–AGTGCTTCTGTGTCTTCG–3′	

Table 1 continued

Gene	Accession no.	Primer (forward/reverse)	Annealing temperature (°C)
Macrophage colony-stimulating factor (MCSF)	NM_023981	5′–ATCCAGGCAGAGACTGACAGA–3′	54.29
		5′–CGCAGTGTAGATGAACCATCC–3′	
Monocyte Chemoattractant Protein-1 (MCP-1)	NM_031530	5′–TGAGTCGGCTGGAGAACTA–3′	51.53
		5′–ATTGGGGTCAGCACAGAT–3′	
Interleukin 1β (IL-1β)	NM_031512	5′–TCAAGCAGAGCACAGACCTGT–3′	56.07
		5′–TGAGAGACCTGACTTGGCAGA–3′	
Interleukin 6 (IL-6)	NM_012589	5′–GCAAGAGACTTCCAGCCAGT–3′	54.97
		5′–AGCCTCCGACTTGTGAAGTG–3′	
Housekeeping gene			
Hypoxanthine phosphoribosyltransferase 1 (Hprt1)	NM_012583	5′–GGCCAGACTTTGTTGGATTTG–3′	53.00
		5′–CTTTCGCTGATGACACAAACAT–3′	

for FAC and FAS, respectively (Fig. 1c). Generally, FAC showed slightly higher inhibitory effects on UMR-106 than FAS.

Both iron species suppressed UMR-106 cell proliferation

UMR-106 osteoblast cells were treated with different concentration of either FAS or FAC at 0, 1, 3, 10, 30, 100, 300 or 1000 μM. Cell proliferation rate was determined by BrdU assay after 24 h of FAC or FAS treatments. The incorporation of BrdU into the newly synthesized DNA represented the ability of cells to proliferate under the treatment of FAS and FAC. FAC showed a more severe effect on UMR-106 cell proliferation (Fig. 2). FAC significantly suppressed UMR-106 cell proliferation by 33.44 and 49.48% at 300 and 1000 μM, respectively (Fig. 2a). On the other hand, FAS significantly inhibited UMR-106 cell proliferation by 26.55% at 100 μM and by 28.53% at 1000 μM. Even though the results were not statistically significant, cells treated with FAS also showed a markedly reduced cell proliferation by 23.43% at 300 μM (Fig. 2b) Corresponding to the results from cell survival assay in Fig. 1, FAC showed the overall greater suppression effects on UMR-106 cell proliferation than FAS.

Ferric and ferrous induced osteoblast cell death

Membrane integrity as well as intracellular enzyme activity can be used to determine cell death and cell viability. In this experiment, cell membrane integrity was assessed by using ethidium homodimer, which penetrated cell and nuclear membrane of the dead cells. After entering the cell, the red-fluorescent ethidium homodimer can bind to DNA inside the cell giving a red fluorescent signal of dead cells. On the other hand, the activity of intracellular esterase to change calcein-AM into the green-fluorescent calcein indicated the viability of living cells. UMR-106 cells were treated with different concentrations of FAC or FAS including 0, 100, 200 and 300 μM for 72 h. After that, the cells were labeled simultaneously with ethidium homodimer and calcein-AM. The intensity of red/green fluorescent signals and the area coverage of green and red fluorescent positive cells were evaluated to get dead/live ratio of each group. Our
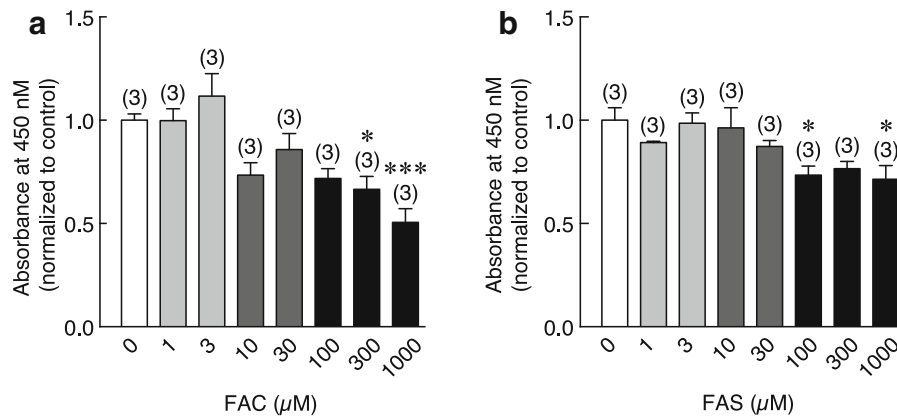
Fig. 2 Both FAC (**a**) and FAS (**b**) suppressed osteoblast cell proliferation as shown by BrdU assay. (*$P < 0.05$, ***$P < 0.001$ as compared to control; experiments were performed in 3 biological replicates each with three technical repeats)

results showed that both iron species induced cell death as indicated by the increased death/live ratio in all treatment groups (Fig. 3a, b). Fluorescent intensity ratios between the red ethidium homodimer (from dead cells) and the green calcein product were 33.50, 34.07 and 35.29 in UMR-106 cells treated with 100, 200 and 300 μM FAS, respectively. Even though the intensity ratios from FAC treated cells were lower than those from FAS treated cells at 28.47 and 24.50 after treated with 100 and 200 μM FAC, respectively, the dead/live intensity ratio was significantly higher to 54.09 with 300 μM FAC (Fig. 3c). The lost of cell membrane integrity of dead cells and the activity of intracellular enzyme of living cells were also measured by the ratios between red fluorescent positive to green fluorescent positive cells representing the ratio between area coverage of the dead cells to living cells. The dead/live ratios were 70.28, 97.43 and 171.32 for cells treated with 100, 200 and 300 μM FAC, respectively. The dead/live ratios were slightly lower for FAS treatment at 65.77, 93.33 and 140.44 for 100, 200 and 300 μM of FAS (Fig. 3d). Taken together, FAC still showed a higher ability to induce osteoblast cell death as indicated by the greater dead/live intensity and dead/live area coverage than FAS.

FAC and FAS induced osteoblast cell death via apoptosis

To investigate the effects of both ferrous and ferric on apoptotic markers level, UMR-106 cells were treated with FAC and FAS for 72 h before collecting protein samples. The samples were used for western blot

analysis of apoptotic markers including cleaved caspase 3 and cleaved caspase 7 to evaluate the protein level of these apoptotic markers after exposing to both iron species (Fig. 4a). Our results showed that the level of cleaved caspase 3 increased drastically after UMR-106 was treated with FAC in a dose-dependent manner (Fig. 4a, b). Although the results were not statically significant, similar trend could be seen in the groups treated with FAS (Fig. 4b). These results suggested that both iron species induced osteoblast cell death via apoptosis pathway. To confirm this speculation, the level of another executioner caspase, cleaved caspase 7, upon the exposure of FAC and FAS was evaluated (Fig. 4a, c). After exposing to FAC, UMR-106 also had a dramatically elevated level of cleaved caspase 7. A slight increase of cleaved caspase 7 could be observed in FAS treated cells (Fig. 4c). Taken together, our results indicated that both ferric and ferrous iron induced osteoblast cell apoptosis with a higher degree from ferric.

FAC and FAS treatments led to increased intracellular iron and gene expression alteration in iron transporters

To determine whether the exposure of both iron treatments led to increased intracellular iron, intracellular iron after 24 h of FAC or FAS treatment was determined by using FAAS. Results from FAAS showed that intracellular iron significantly elevated after FAC treatment from 0.18 mg iron/mg proteins in the control to 0.43, 0.65 and 1.03 mg iron/mg proteins after treated with 100, 200 and 300 μM of FAC.
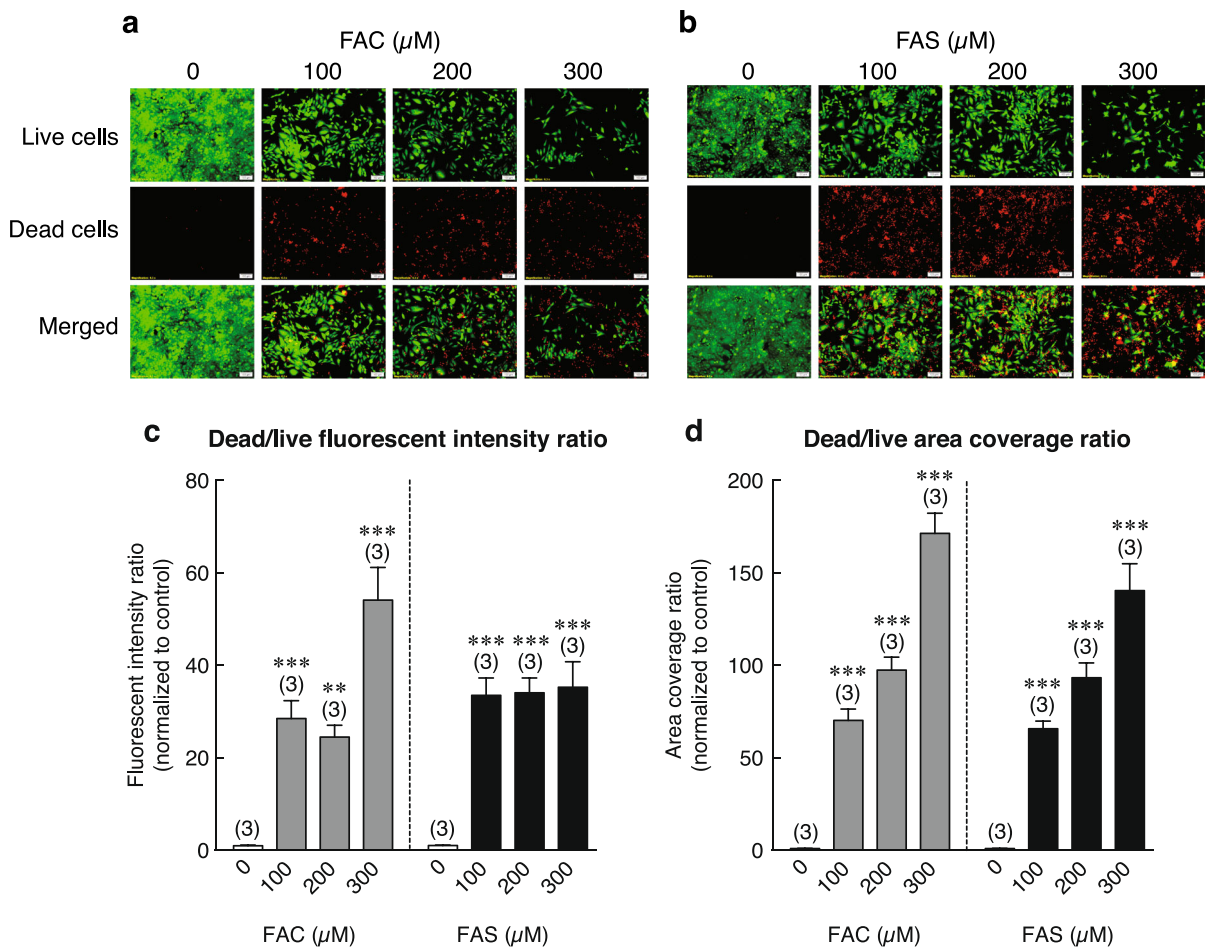
Fig. 3 The dead-inducing activity from FAC and FAS on osteoblast UMR-106 was tested by live/dead assay. Green fluorescent signal from calcein stained live cells, and red fluorescent signal from ethidium homodimer stained dead cells. UMR-106 cells treated with FAC (**a**) and FAS (**b**) showed decreased live cells and increased dead cells in dose-dependent manner. The quantified data from dead/live fluorescent intensity ratio (**c**) and dead/live area coverage ratio (**d**) confirmed the elevation of dead cell population and the reduction of live cell population in UMR-106 cells treated with FAC and FAS. (**P < 0.01, ***P < 0.001 as compared to control; experiments were performed in 3 biological replicates each with 7–8 technical repeats). (Color figure online)

Likewise, intracellular iron increased from 0.17 mg iron/mg proteins in the control group to 0.56, 0.50, 0.51 for 100, 200 and 300 μM FAS treated cells (Fig. 5a). Our results indicated that FAC induced higher intracellular iron uptake in osteoblast cells as compared to FAS.

To examine the potential transporter(s) responsible for cellular transport of iron in osteoblasts, the expression level of iron transport machineries upon FAC and FAS treatment was investigated by qRT-PCR. After 72-h iron treatment, iron transporters and its associated genes showed gene expression alterations after iron exposure (Fig. 5b–i). Results showed

that the DMT1 levels were reduced by 56 and 45% after FAC and FAS treatment, respectively (Fig. 5b). Similar trend could be seen in genes for transferrin receptor 1 and 2 (TfR1 and TfR2) with approximately 70 and 20% reduction for TfR1 and TfR2 after both iron treatments (Fig. 5c, d). Only minor reduction was observed in Dcytb gene expression after FAC and FAS treatment (Fig. 5e). On the other hand, the opposite trend was observed for hephaestin (Heph) and Fpn. Specifically, Heph expression was upregulated by 1.38- and 1.18-fold for FAC and FAS (Fig. 5f), while the expression levels of Fpn were increased significantly by 1.71- and 1.36-fold as compared to control
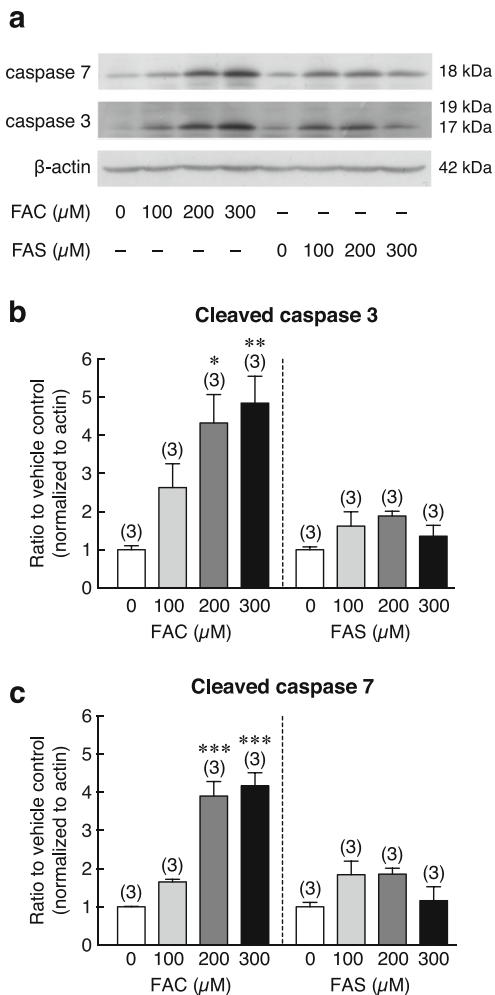
a

b

c

Fig. 4 The representative blot showed the elevation of cleaved caspase 3 and cleaved caspase 7 in UMR-106 exposed to FAC and FAS (**a**). The quantified data showed a significant increase in cleaved caspase 3 (**b**) and cleaved caspase 7 (**c**) in UMR-106 treated with FAC. Even though the results were not statistically significant, similar trend could be seen in UMR-106 treated with FAS. (*$P < 0.05$, **$P < 0.01$, ***$P < 0.001$ as compared to control; experiments were performed in three biological replicates)

(Fig. 5h). There were no significant changes in hemochromatosis protein (HFE) and Cp (Fig. 5g, i), but the latter of which showed a tendency of upregulation.

Both iron species decreased alkaline phosphatase (ALP) activity

Comparative effects of FAS and FAC on osteoblast differentiation and activity were determined by the

activity of ALP. After treated with either FAC or FAS at 100, 200 or 300 μM for 24 h, ALP activity from UMR-106 cells was assessed. The activity of ALP and the activity of ALP normalized to protein content were evaluated. Our results showed a significant decrease in ALP activity from UMR-106 treated with FAC (Fig. 6a). Similar trend could be found in UMR-106 treated with FAS (Fig. 6b). When the activity of ALP was normalized to protein content of each sample, the results were quite fluctuated. However, the reduction of ALP in UMR-106 treated with 300 μM of FAC and FAS were clearly seen (Fig. 6c, d). Our overall results showed that both FAC and FAS, especially the high dose treatment, suppressed ALP activity in UMR-106 cells.

Ferrous and ferric differently affected osteoblastic and osteoclastogenic genes expression

In addition to the expression of osteoblastic genes that directly promote osteoblast differentiation itself, osteoblast also regulates osteoclast differentiation and activity through the interaction and secretion of several osteoblastic and osteoclastogenic factors. Here, the expression levels of osteoblastic genes that promote osteoblast differentiation, but inhibit osteoclast differentiation were determined (Fig. 7). Results showed that the expression levels of erythropoietin-producing human hepatocellular receptor-interacting protein B2 (Ephrin B2), Cyclooxygenase 2 (Cox-2) and osteoprotegerin (OPG) were 1.06, 1.70 and 1.44 fold increased after FAC treatment relative to control (Fig. 7a, c–d). While there was no significant change in erythropoietin-producing human hepatocellular receptors B4 (Eph B4) after FAC treatment, FAS treatment led to a downregulation of Ephrin B2 and Eph B4 by 16 and 25% as compared to control (Fig. 7a, b). The small increase in COX-2 and OPG expression was seen after FAS treatment (Fig. 7c, d). Additional experiments were performed for 2 early differentiation markers, i.e., *Runt*-related transcription factor 2 (Runx2) and osteocalcin (OCN) using rat β-actin as a housekeeping gene. However, when UMR-106 cells were treated with 100 μM of FAC and FAS, the expression of the two markers was not significantly altered ($P > 0.05$; n = 6/group). Specifically, the Runx2 expression showed only 1.01 ± 0.16 ($P = 0.998$) and 1.04 ± 0.14 ($P = 0.99$) fold as compared to control in FAC- and FAS-treated groups,
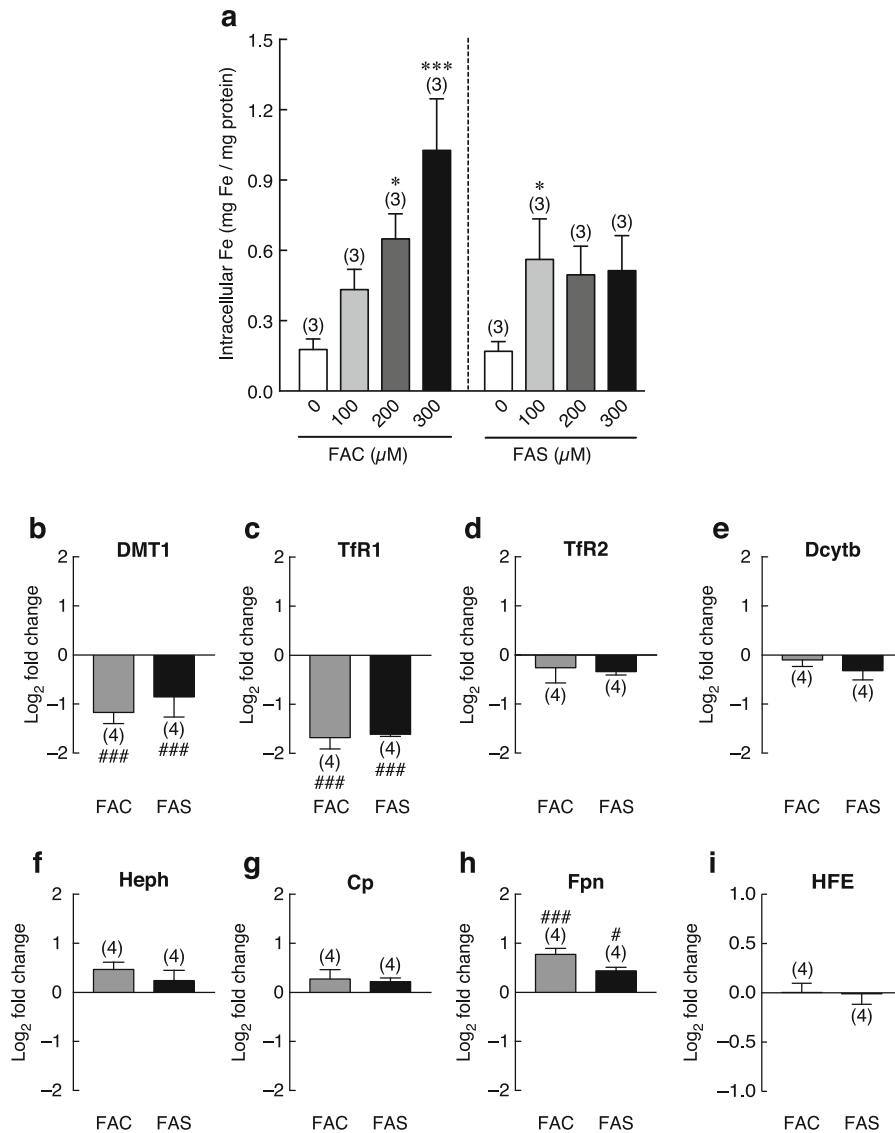
Fig. 5 a FAC and FAS treatment on UMR-106 cells led to elevated intracellular iron in dose-dependent manner. $*P < 0.05$, $***P < 0.001$ as compared to control; experiments were performed in 3 biological replicates each with three technical repeats. **b–i** Gene expression alteration of iron transporters and proteins functioning in cellular iron transport after iron exposure at the IC$_{50}$ obtained from Fig. 1 (221.64 μM for FAC and 232.35 μM for FAS) compared with the control group. The expression of DMT1 (**b**), TfR1 (**c**), TfR2 (**d**) and Dcytb (**e**) in UMR-106 was reduced after both FAC and FAS exposure. The expression of Heph (**f**), Cp (**g**), Fpn (**h**) was induced with FAC and FAS treatment; while HFE was unaffected (**i**). $^{\#}P < 0.05$, $^{\#\#\#}P < 0.001$ as compared to control group; experiments were performed in four biological replicates each with three technical repeats

respectively. The OCN expression levels were 1.13 ± 0.25 ($P = 0.467$) and 1.25 ± 0.19 ($P = 0.539$) fold in FAC and FAS treated groups as compared to the control group. On the other hand, expression levels of osteoclastogenic genes, which promote osteoclast differentiation, were also tested.

Our data showed that FAC treatment led to a significantly increase in monocyte chemotactic protein 1 (MCP-1) and interleukin 6 (IL-6) to 2.80 and 2.14 fold change normalized to control (Fig. 7e, f). FAC showed only a minimal effect on macrophage colony-stimulating factor (M-CSF) and interleukin-1β
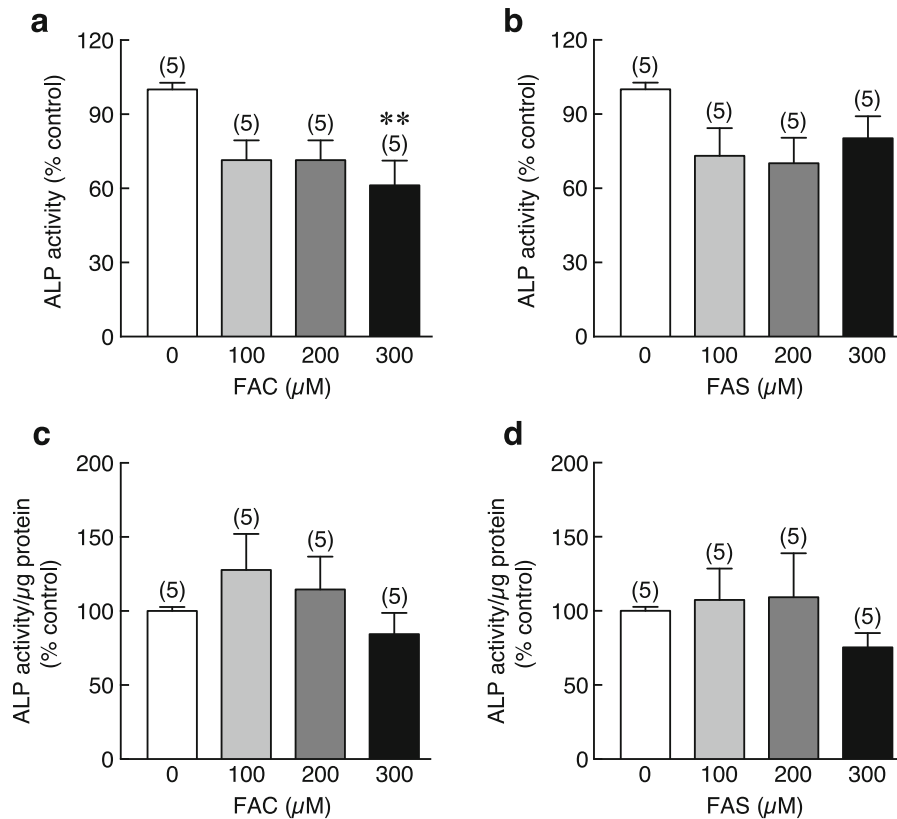
Fig. 6 ALP activity from UMR-106 cells treated with FAC and FAS was determined. ALP activity in UMR-106 cells was significantly reduced after 24 h of FAC treatment (**a**). Similar trend was observed in UMR-106 cells treated with FAS (**b**). When ALP activity was normalized to protein content of each sample, the decreased ALP activity in UMR-106 treated was seen in cells treated with 300 μM FAC and FAS (**c**, **d**). (**$P < 0.01$ as compared to control; experiments were performed in 5 biological replicates each with three technical repeats)

(IL-1β) (Fig. 7g, h). Interestingly, FAC significantly suppressed Receptor activator of nuclear factor κB ligand (RANKL) expression (Fig. 7i). On the other hand, FAS induced an increased expression of MCP-1 and IL-6 to 1.87 and 1.378 fold change relative to control (Fig. 7e, f). The expression of MCSF, IL-1β and RANKL was minimally altered after FAS treatment.

Discussion

As a pivotal element for human body, excess amount of iron or iron overload can be deleterious to many organs including bone. Iron overload could come from uncontrollable iron absorption as in hemochromatosis as well as from increased iron absorption or repeated blood transfusion to compensate with ineffective erythropoiesis in several blood diseases, such as β-thalassemia. It has been demonstrated that iron had negative effects on bone structure and calcium home-ostasis, presumably by enhancing bone resorption and suppressing bone formation, the latter of which might be related to the ferroxidase activity of ferritin (Chen et al. 2015; Tian et al. 2016; Tsay et al. 2010; Zarjou et al. 2010; Zhao et al. 2014). Bone formation was found to have an inverse correlation with degree of iron overload (Diamond et al. 1991; Tsay et al. 2010). Iron overload was also associated with reduced osteoblast recruitment and collagen synthesis in osteoporotic pig (de Vernejoul et al. 1984). While the normal serum iron levels range from 10 to 30 μM, the concentration can be elevated to > 50 μM in iron-overloaded patients (Ganz 2007; Zhao et al. 2014). In addition, serum iron > 89.5 μM can cause serious systemic toxicity, and mortality rate is high when

Fig. 7 Gene expression levels of osteoblastic and osteoclastogenic genes in UMR-106 after being treated with FAC and FAS at the IC_{50} obtained from Fig. 1 (221.64 μM for FAC and 232.35 μM for FAS) compared with the control group. The osteoblastic genes including Ephrin B2 (**a**), Eph B4 (**b**), Cox-2 (**c**), OPG (**d**) MCP-1 (**e**), IL-6 (**f**), MCSF (**g**), IL-1β (**h**) and RANKL (**i**) were studied. OPG, Cox-2, MCP-1 and IL-6 were significantly increased with FAC treatment. IL-6 expression was also induced by FAS. RANKL expression was suppressed by FAC. $^{\#}P < 0.05$, $^{\#\#}P < 0.01$, $^{\#\#\#}P < 0.001$ as compared to control; experiments were performed in four biological replicates each with three technical repeats
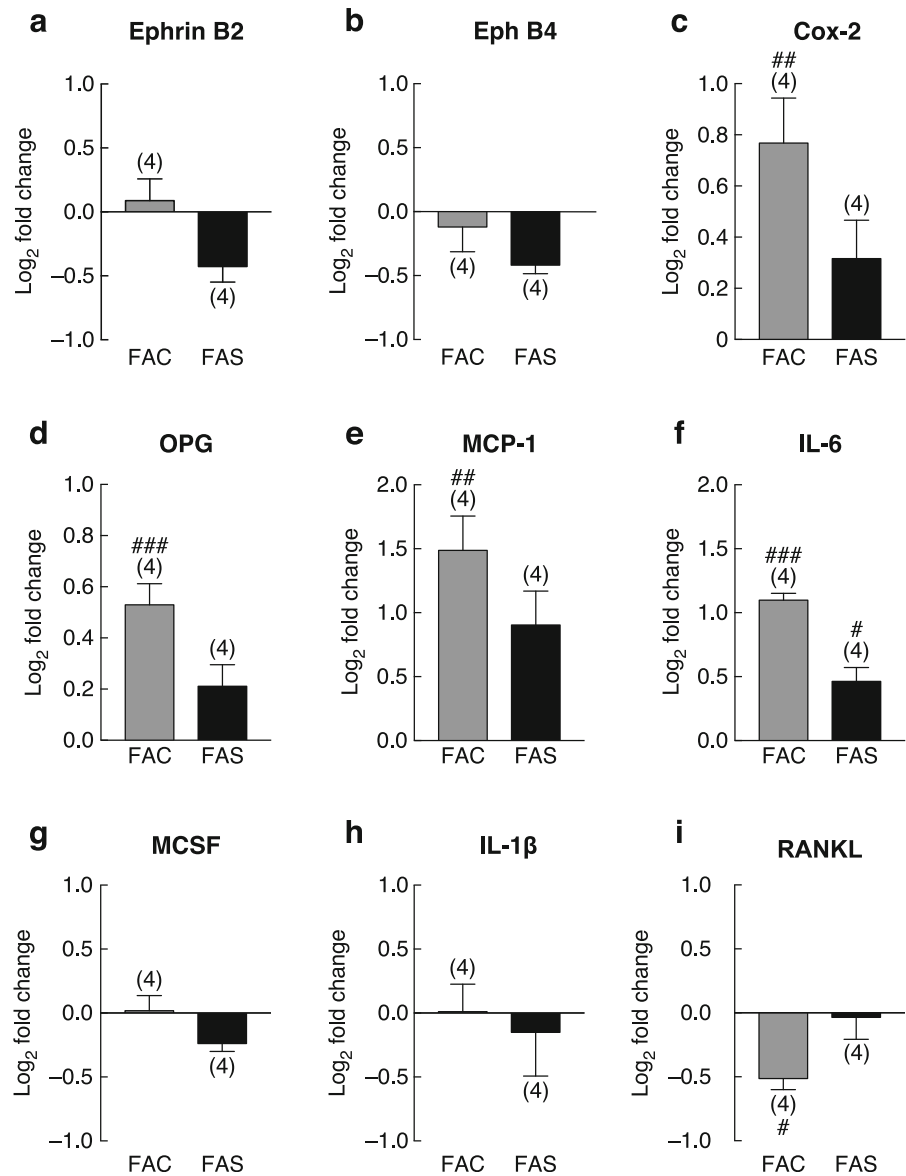
serum iron > 179 μM (Bregstein et al. 2011). Thus, the investigation of effects of iron on osteoblasts in the present study was performed in the broad range of iron concentration (0–1 mM) to investigate the effects of both physiological and supra-physiological concentrations, some of which (e.g., 100 μM) could be observed in iron-overloaded conditions.

Two major forms of iron exist in biological systems, i.e., ferrous (Fe^{2+}) and ferric (Fe^{3+}). In this study, FAS and FAC were used to study the differential effects of the two iron species on osteoblast cell survival and proliferation. The results showed that both FAC and FAS suppressed osteoblast cell survival in dose and time-dependent manner (Fig. 1a–c). Similarly, data from BrdU assay indicated that high dosage of both iron species significantly decreased osteoblast cell proliferation even within 24 h (Fig. 2). Our results corresponded to previous studies showing negative effects of iron on osteoblast cells (Balogh et al. 2016; Diamond et al. 1991; He et al. 2013; Messer et al. 2009; Tian et al. 2016; Yamasaki and Hagiwara 2009; Zhang et al. 2017). It has been shown that ferrous sulfate treatment caused osteoblast cell death in fetal rat-derived calvarial culture (Messer

et al. 2009). In addition, a high-dose ferric nitrate and FAC suppressed osteoblast cell proliferation and decreased cell viability of mouse osteoblast-like MC3T3-E1 cells (Diamond et al. 1991; Yamasaki and Hagiwara 2009). In addition to the similar anti-proliferative effects of iron on osteoblasts as reported before and in this study, this is the very first study to compare the effects of ferrous and ferric iron on osteoblast cell survival and proliferation. Our results have suggested that ferric from FAC has more detrimental effects on osteoblast cell survival and cell proliferation than ferrous from FAS (Figs. 1, 2).

To verify whether both iron species also induced osteoblast cell death, the measurement of the lost of membrane integrity and the activity of intracellular esterase representing dead and live cells were performed. Our results showed the dramatically elevated dead/live intensity ratio and dead/live area coverage in UMR-106 after both iron treatments with the stronger effects from FAC than FAS (Fig. 3). This indicated that both iron species induced osteoblastic cell death with the higher death-inducing effect from ferric than ferrous. Thus, in the presence of high circulating iron from intestinal iron hyperabsorption as in thalassemia and hemochromatosis, it could potentially cause a deleterious effect on osteoblasts, leading to iron overload-associated osteopathy.

While both iron species could induce osteoblast cell death, the mechanism behind this phenomenon is still unknown. Since the cleavage of executioner caspases, i.e., caspase 3 and 7, is widely accepted as a hallmark for apoptosis (Bressenot et al. 2009), protein levels of these apoptotic markers were investigated (Fig. 4). In this study, the level of cleaved caspase 3 was markedly elevated in osteoblasts treated with FAC and slightly increased in osteoblasts treated with FAS. This confirmed that both iron species induced osteoblast apoptosis with a stronger effect from ferric. These results were consistent with the previous studies reported the effects of FAC to induce osteoblast apoptosis (Ke et al. 2017; Liu et al. 2017; Tian et al. 2016). Our data revealed notable changes in cleaved apoptotic markers from ferric treatment versus the slight changes from ferrous treatment. However, the two iron species showed similar IC_{50} and had relatively resembling dead/live cell ratio for UMR-106 cells, suggesting that the two iron species might use different pathways to induce osteoblast cell death.

To demonstrate whether these iron treatments led to an increase in intracellular iron in osteoblasts, intracellular iron was measured after each iron exposure. Our results showed that upon the exposure of both ferric and ferrous treatments, the intracellular iron was remarkably increased (Fig. 5a). It is worth mentioning that FAC induced significantly higher intracellular iron in osteoblast treated with FAS at the same concentration. In other words, the transport of ferric iron across the plasma membrane of osteoblasts might be easier than that of ferrous iron. In contrast to the well-known mechanisms in enterocytes, iron transport mechanism in osteoblasts remains unclear. Gene expression of some iron-transporting proteins was thus verified in this study. Our results showed that osteoblast-like UMR-106 cells strongly expressed DMT1, TfR1, TfR2, Dcytb, Fpn, Heph, Cp and HFE. As we tested for the gene expression alteration of iron transporter genes in osteoblasts after FAC and FAS treatments, the results were consistent between the two iron species. Interestingly, our data showed that iron transporters, which are responsible for iron uptake mechanisms including DMT1, DCytb, TfR1 and TfR2, were significantly downregulated. In contrast, the expression of iron transporters involving in iron export mechanism, including Fpn1, HEph and Cp was upregulated. Our results are different from the previous study that showed an increase in DMT1 expression in 24-h FAC-treated hFOB1.19 fetal osteoblasts (Liu et al. 2017). Corresponding to our data, results from another group also showed that FAC treatment induced the iron exporter, Fpn1 expression in human hFOB1.19 osteoblasts (Zhao et al. 2014). Since our study and others showed that iron induced osteoblast cell death with the strong correlation with increased intracellular iron (Fig. 5a) (Tian et al. 2016), such adaptation to increase iron export but decrease iron import could potentially provide the survival advantages to iron-overloaded osteoblasts. Although a downregulation of ferrous-transporting DMT1 expression may explain as to why ferrous was less toxic than ferric, more investigation is required to reveal how osteoblasts uptake ferric into the cytoplasm and why ferric accumulation is more robust.

Furthermore, the possible effects of both ferrous and ferric on osteoblast differentiation were tested in this study. Our results showed a marked decrease in ALP activity after treatment with ferric or ferrous for 24 h (Fig. 5). Similar to previous characteristics, the

higher significant effects could be seen from ferric treatment (FAC) than from ferrous treatment (FAS). Our findings corresponded to previous studies that illustrated the negative effects of ferric on osteoblast-derived ALP activity (Diamond et al. 1991; He et al. 2013; Jeney 2017; Yamasaki and Hagiwara 2009; Zhao et al. 2012). Furthermore, FAC and ferritin ferroxidase have been shown to inhibit osteoblast differentiation and extracellular matrix calcium deposition in human osteosarcoma 143-B cells, indicating the potential mechanism of iron-mediated osteoblast differentiation and suppression of matrix mineralization by ferritin ferroxidase activity (Zarjou et al. 2010). Herein, we reported similar phenomenon and the comparative effects of ferric and ferrous on rat osteoblast-like UMR-106 cells.

Under normal conditions, bone homeostasis is regulated by the process called bone-remodeling process, which is governed by the activity of bone-forming cells (osteoblasts) and bone-resorbing cells (osteoclasts). To keep the balance remodeling process, the development and functionalities of these cells are determined by the signals from itself as well as the interplay signals from another cell type. The combinations of the intracellular signals and extracellular signals will determine whether the bone will be formed or removed by the responsible cells (Proff and Romer 2009; Raggatt and Partridge 2010). Normally, several systems, e.g., RANKL-OPG, Ephrin-Eph and Cox-2, plays important roles in this bone-remodeling process. The expression alterations of osteoblast-derived osteoblastic genes that facilitate bone formation by osteoblast and osteoblast-derived osteoclastogenic genes that regulate bone resorption by osteoclast upon iron exposure was also determined (Fig. 7). Osteoblastic gene markers used in this study included Cox-2, OPG, Ephrin B2 and Eph4. Our results showed that both iron species moderately increased the expression of Cox-2 and OPG. Since Cox-2 also plays an important role in inflammatory responses of the cells under stress, an enhanced expression of Cox-2 was also found in several cell types in response to iron-induced stress, such as hepatocytes and brain cells (Lee et al. 2010; Lukiw and Bazan 1998; Salvador et al. 2010). However, both iron forms led to a decrease in Eph B4 expression, whereas only FAS suppressed the expression of Ephrin B2. Therefore, differential expression alterations of several osteoblastic genes in osteoblast cell

treated with iron were found in our study. It is worth mentioning that ferrous and ferric showed different degree of gene expression induction/suppression with an opposite effect on Ephrin B2. As many studies reported about the direct effects of iron on osteoclast differentiation, the effects on osteoblast-derived osteoclastogenic factor expression are still limited (Guo et al. 2015; Xiao et al. 2015, 2018; Xie et al. 2016). In this study, the expression change of the osteoclastogenic genes including MCSF, MCP-1, IL-1β and IL-6 after iron exposure to osteoblast was determined in this study. While the slightly reduced expression of MCSF and IL-1β and moderately lower expression of RANKL were observed in osteoblast treated with iron, both iron species markedly induced the expression of MCP-1 and IL-6 in osteoblast cells. Osteoblast is known to secrete these cytokines to facilitate osteoclast differentiation and activity (Boyle et al. 2003; Cappellen et al. 2002; Matsuo and Irie 2008). As mentioned earlier, the combination of osteoblastic factors and osteoclastogenic factors would determine the phase of bone remodeling process. Even though iron treatments induced the expression of a few osteoblastic genes in osteoblast UMR-106 cells, the opposite effects were also seen in some other osteoblastic genes. Additionally, the greater enhancement was observed in some osteoclastogenic genes after iron exposure in this study. These gene expression alterations implied the shifting role of osteoblast to induce bone resorption rather than bone formation during iron overload. Taken together, our results explained the direct effects of iron on osteoblast cells itself and the indirect effects on osteoblast-mediated osteoclast differentiation during overload-induced osteoporosis. Similar to other experiments in this study, ferric still showed the overall stronger effects on osteoblast gene expression alterations than ferrous (Fig. 7).

Our data suggested the differential contribution of the two iron species in iron overload-induced osteoporosis as ferric showed the overall greater effects on osteoblasts than ferrous. Fenton reaction has been used to explain iron toxicity in many cells. In this reaction, ferrous and ferric react with hydrogen peroxide to generate reactive oxygen species including hydroxyl radical ($\bullet$OH) and hydroperoxyl radical ($HO_2\bullet$) causing DNA and cell structural damage (Djordjevic 2004; Salgado et al. 2013; Winterbourn 1995). It has been shown that hydroxyl radical produced from Fenton

reaction of ferrous or copper is the most reactive radical known (Djordjevic 2004). With this principle, ones might assume that ferrous should be more toxic than ferric for the cells. However, our results showed that ferric treatment caused significantly higher intracellular iron in osteoblast than ferrous treatment (Fig. 5a). These results indicated that osteoblasts have the greater sensitivity to ferric than ferrous potentially by the higher level of iron transported into the cytoplasm. Accordingly, our study implied that ferric iron from the increased iron absorption (as observed in thalassemia) has greater deleterious impact on osteoblasts than ferrous iron from blood transfusion in iron-overloaded thalassemic patients. The results from this study would be beneficial for the development of interventions and iron chelation treatment for iron-induced osteoporosis.

Compliance with Ethical Standards

Conflict of interest   The authors declare that there is no conflict of interest.

References

Balogh E, Tolnai E, Nagy B Jr, Nagy B, Balla G, Balla J, Jeney V (2016) Iron overload inhibits osteogenic commitment and differentiation of mesenchymal stem cells via the induction of ferritin. Biochim Biophys Acta 1862:1640–1649. https://doi.org/10.1016/j.bbadis.2016.06.003

Boyle WJ, Simonet WS, Lacey DL (2003) Osteoclast differentiation and activation. Nature 423:337–342. https://doi.org/10.1038/nature01658

Bregstein J, Roskind CG, Sonnett FM (2011) CHAPTER 5—emergency medicine A2—Polin, Richard A. In: Ditmar MF (ed) Pediatric secrets, 5th edn. Mosby, Philadelphia, pp 154–196. https://doi.org/10.1016/B978-0-323-06561-0.00005-7

Bressenot A, Marchal S, Bezdetnaya L, Garrier J, Guillemin F, Plenat F (2009) Assessment of apoptosis by immunohistochemistry to active caspase-3, active caspase-7, or cleaved PARP in monolayer cells and spheroid and subcutaneous xenografts of human carcinoma. J Histochem

Cytochem 57:289–300. https://doi.org/10.1369/jhc.2008.952044

Cappellen D, Luong-Nguyen NH, Bongiovanni S, Grenet O, Wanke C, Susa M (2002) Transcriptional program of mouse osteoclast differentiation governed by the macrophage colony-stimulating factor and the ligand for the receptor activator of NFkappa B. J Biol Chem 277:21971–21982. https://doi.org/10.1074/jbc.M200434200

Chen B, Li GF, Shen Y, Huang XI, Xu YJ (2015) Reducing iron accumulation: a potential approach for the prevention and treatment of postmenopausal osteoporosis. Exp Ther Med 10:7–11. https://doi.org/10.3892/etm.2015.2484

de Vernejoul MC, Pointillart A, Golenzer CC, Morieux C, Bielakoff J, Modrowski D, Miravet L (1984) Effects of iron overload on bone remodeling in pigs. Am J Pathol 116:377–384

Diamond T, Pojer R, Stiel D, Alfrey A, Posen S (1991) Does iron affect osteoblast function? Studies in vitro and in patients with chronic liver disease. Calcif Tissue Int 48:373–379

Djordjevic VB (2004) Free radicals in cell biology. Int Rev Cytol 237:57–89. https://doi.org/10.1016/S0074-7696(04)37002-6

Ganz T (2007) Molecular control of iron transport. J Am Soc Nephrol: JASN 18:394–400. https://doi.org/10.1681/ASN.2006070802

Guo JP, Pan JX, Xiong L, Xia WF, Cui S, Xiong WC (2015) Iron chelation inhibits osteoclastic differentiation in vitro and in Tg2576 mouse model of Alzheimer's disease. PLoS ONE 10:e0139395. https://doi.org/10.1371/journal.pone.0139395

He YF et al (2013) Iron overload inhibits osteoblast biological activity through oxidative stress. Biol Trace Elem Res 152:292–296. https://doi.org/10.1007/s12011-013-9605-z

Jeney V (2017) Clinical impact and cellular mechanisms of iron overload-associated bone loss. Front Pharmacol 8:77. https://doi.org/10.3389/fphar.2017.00077

Ke JY, Cen WJ, Zhou XZ, Li YR, Kong WD, Jiang JW (2017) Iron overload induces apoptosis of murine preosteoblast cells via ROS and inhibition of AKT pathway. Oral Dis 23:784–794. https://doi.org/10.1111/odi.12662

Lee FP, Jen CY, Chang CC, Chou Y, Lin H, Chou CM, Juan SH (2010) Mechanisms of adiponectin-mediated COX-2 induction and protection against iron injury in mouse hepatocytes. J Cell Physiol 224:837–847. https://doi.org/10.1002/jcp.22192

Liu F, Zhang WL, Meng HZ, Cai ZY, Yang MW (2017) Regulation of DMT1 on autophagy and apoptosis in osteoblast. Int J Med Sci 14:275–283. https://doi.org/10.7150/ijms.17860

Lukiw WJ, Bazan NG (1998) Strong nuclear factor-kappaB-DNA binding parallels cyclooxygenase-2 gene transcription in aging and in sporadic Alzheimer's disease superior temporal lobe neocortex. J Neurosci Res 53:583–592. https://doi.org/10.1002/(SICI)1097-4547(19980901)53:5<583::AID-JNR8>3.0.CO;2-5

MacKenzie EL, Iwasaki K, Tsuji Y (2008) Intracellular iron transport and storage: from molecular mechanisms to health implications. Antioxid Redox Signal 10:997–1030. https://doi.org/10.1089/ars.2007.1893

Matsuo K, Irie N (2008) Osteoclast-osteoblast communication. Arch Biochem Biophys 473:201–209. https://doi.org/10.1016/j.abb.2008.03.027

McKie AT et al (2001) An iron-regulated ferric reductase associated with the absorption of dietary iron. Science 291:1755–1759. https://doi.org/10.1126/science.1057206

Messer JG, Kilbarger AK, Erikson KM, Kipp DE (2009) Iron overload alters iron-regulatory genes and proteins, down-regulates osteoblastic phenotype, and is associated with apoptosis in fetal rat calvaria cultures. Bone 45:972–979. https://doi.org/10.1016/j.bone.2009.07.073

Noble JE, Bailey MJ (2009) Quantitation of protein. Methods Enzymol 463:73–95. https://doi.org/10.1016/S0076-6879(09)63008-1

Proff P, Romer P (2009) The molecular mechanism behind bone remodelling: a review. Clin Oral Investig 13:355–362. https://doi.org/10.1007/s00784-009-0268-2

Raggatt LJ, Partridge NC (2010) Cellular and molecular mechanisms of bone remodeling. J Biol Chem 285:25103–25108. https://doi.org/10.1074/jbc.R109.041087

Salgado P, Melin V, Contreras D, Moreno Y, Mansilla HD (2013) Fenton reaction driven by iron ligands. J Chil Chem Soc 58:2096–2101. https://doi.org/10.4067/S0717-97072013000400043

Salvador GA, Uranga RM, Giusto NM (2010) Iron and mechanisms of neurotoxicity. Int J Alzheimers Dis 2011:720658. https://doi.org/10.4061/2011/720658

Tian Q, Wu S, Dai Z, Yang J, Zheng J, Zheng Q, Liu Y (2016) Iron overload induced death of osteoblasts in vitro: involvement of the mitochondrial apoptotic pathway. PeerJ 4:e2611. https://doi.org/10.7717/peerj.2611

Tsay J et al (2010) Bone loss caused by iron overload in a murine model: importance of oxidative stress. Blood 116:2582–2589. https://doi.org/10.1182/blood-2009-12-260083

Winterbourn CC (1995) Toxicity of iron and hydrogen peroxide: the Fenton reaction. Toxicol Lett 82–83:969–974

Xiao W, Beibei F, Guangsi S, Yu J, Wen Z, Xi H, Youjia X (2015) Iron overload increases osteoclastogenesis and aggravates the effects of ovariectomy on bone mass. J Endocrinol 226:121–134. https://doi.org/10.1530/JOE-14-0657

Xiao W et al (2018) Iron-induced oxidative stress stimulates osteoclast differentiation via NF-kappaB signaling pathway in mouse model. Metabolism. https://doi.org/10.1016/j.metabol.2018.01.005

Xie W, Lorenz S, Dolder S, Hofstetter W (2016) Extracellular iron is a modulator of the differentiation of osteoclast lineage cells. Calcif Tissue Int 98:275–283. https://doi.org/10.1007/s00223-015-0087-1

Yamasaki K, Hagiwara H (2009) Excess iron inhibits osteoblast metabolism. Toxicol Lett 191:211–215. https://doi.org/10.1016/j.toxlet.2009.08.023

Zarjou A, Jeney V, Arosio P, Poli M, Zavaczki E, Balla G, Balla J (2010) Ferritin ferroxidase activity: a potent inhibitor of osteogenesis. J Bone Miner Res 25:164–172. https://doi.org/10.1359/jbmr.091002

Zhang D, Wong CS, Wen C, Li Y (2017) Cellular responses of osteoblast-like cells to 17 elemental metals. J Biomed Mater Res A 105:148–158. https://doi.org/10.1002/jbm.a.35895

Zhao GY, Zhao LP, He YF, Li GF, Gao C, Li K, Xu YJ (2012) A comparison of the biological activities of human osteoblast hFOB1.19 between iron excess and iron deficiency. Biol Trace Elem Res 150:487–495. https://doi.org/10.1007/s12011-012-9511-9

Zhao GY, Di DH, Wang B, Zhang P, Xu YJ (2014) Iron regulates the expression of ferroportin 1 in the cultured hFOB 1.19 osteoblast cell line. Exp Ther Med 8:826–830. https://doi.org/10.3892/etm.2014.1823